SINTECHCOM: Science, Technology and Communication Journal
Vol. 6, No. 3, June 2026, pp. 255-270, DOI: 10.59190/stc.v6i3.382

Adsorption of lead (II) ions using NaOH-activated matoa fruit shell (*Pometia pinnata*): Characterization and adsorption kinetics

Fadhil Maulana Harahap, T. Abu Hanifah, Sofia Anita*
Department of Chemistry, Universitas Riau, Pekanbaru 28293, Indonesia

ABSTRACT

This study focuses on the utilization of matoa fruit shell waste, which contains cellulose, as a potential biosorbent for binding heavy metals in solution. The study aims to examine the ability of matoa fruit shell powder (*Pometia pinnata*) as a biosorbent in removing lead (II) ions from solution and to analyze adsorption characteristics through kinetic studies. The research methods included biosorbent activation using NaOH at activation ratios of 1:1, 1:2, 1:3, 1:4, and 1:5 (w/v). The adsorption process was conducted with variations in parameters, including biosorbent dose, pH, and contact time. Characterization was performed using FTIR to determine functional groups, SEM-EDS to examine surface morphology and elemental composition, and ICP-OES to determine lead concentration in the solution. Kinetic analysis employed first-order pseudo-kinetic, second-order pseudo-kinetic, and intraparticle diffusion models. FTIR analysis results indicated the involvement of hydroxyl (-OH) and carboxyl ($-COO^-$) groups in the lead (II) ion binding process. The results of the study indicate that optimal adsorption conditions were achieved at a dose of 0.05 grams, a pH of 6, and a contact time of 60 minutes, with an adsorption efficiency of 90.76% and an adsorption capacity of 27.59 mg/g. The most suitable kinetic model was the pseudo-second-order model (R^2 = 0.9999), indicating a chemisorption mechanism.

ARTICLE INFO

Article history:

Received Jun 10, 2026
Revised Jun 13, 2026
Accepted Jun 14, 2026

Keywords:

Adsorption Kinetics
Biosorbent
Lead (II) Ions
Matoa Fruit Shell
NaOH Activation

* **Corresponding Author**
E-mail address: sofia.anita@lecturer.unri.ac.id

1. INTRODUCTION

Indonesia Indonesia is a country with immense biodiversity, one of which comes from the matoa plant (*Pometia pinnata*), which belongs to the *Sapindaceae* family. This plant is endemic to Irian Jaya and Papua, but has now spread widely to various regions of Indonesia such as Sumatra, Java, Kalimantan, Sulawesi, Sumbawa Island (NTB), and Maluku [1]. Matoa consists of three cultivars based on skin color: green matoa (*Emme Anokhong*), yellow matoa (*Emme Khabelaw*), and red matoa (*Emme Bhanggahe*). These three cultivars share similar morphological characteristics. Research conducted by Yuniastuti et al. (2023) showed that DNA band pattern analysis using the RAPD method revealed that green and yellow matoa are genetically closer, with a coefficient of 0.698, while the greatest genetic distance is between yellow and red matoa, with a coefficient of 0.566 [2].

The matoa plant has long been used by Asian peoples, particularly in Papua, Malaysia, and Indonesia, as a traditional medicine [3]. Research on phytochemical screening of a 96% ethanol extract from matoa leaves revealed the presence of alkaloids, flavonoids, tannins, steroids, and triterpenoids [4]. Some of the reported benefits of the matoa plant include treatment for burns, stomach disorders, diarrhea, dysentery, muscle, bone, and joint pain, as well as for the common cold, flu, and diabetes [3]. Research conducted by Pakaya et al. (2021) examined the use of matoa fruit peel waste as a herbal mouthwash for the prevention of dental caries [5]. Meanwhile, Faustina and Santoso (2014) had previously utilized matoa fruit peel for extraction and the assessment of antioxidant and

antimicrobial activities [6]. However, the utilization of matoa fruit peel remains limited to this day and is often simply discarded as waste. Matoa fruit peel has the potential to serve as a biosorbent for heavy metal waste, particularly lead. This study focuses on the utilization of green matoa fruit peel because it is easier to obtain and widely found in Perawang Subdistrict, Siak Regency, Riau, which constitutes the study area.

Currently, various types of biosorbents have been developed to adsorb heavy metals. One such method utilizes cellulose, which possesses active functional groups capable of binding with lead metal ions [7]. Matoa fruit peel is known to have a fairly high cellulose content, around 50.6%, even exceeding the cellulose content in other materials such as rice straw (27% – 34%) and sugarcane bagasse (36% – 40%) [8]. This high cellulose content indicates that matoa fruit peel has potential as a raw material for biosorbent production because it contains a large amount of carbon. The higher the carbon content, the better a material's ability to function as a biosorbent [9].

Adsorption is a process in which an adsorbate accumulates on the surface of an adsorbent (biosorbent) due to attractive forces, whether through physisorption or chemisorption [10]. According to Hughes & Poule (1984), the adsorption process via ion exchange and complexation occurs only on the surface layer of cells that possess sites with charges opposite to those of heavy metal ions, resulting in passive and relatively rapid interactions [11]. The adsorption method is used because it offers advantages, such as relatively low cost, relatively high adsorption effectiveness and efficiency, a simple process, and no side effects in the form of toxic substances [12]. Faza (2021) used matoa fruit peel as a biosorbent activated with 1 M nitric acid, varying pH, contact time, and concentration. The results of the characterization of the optimal activated carbon in this study according to SNI 06-3730-1995 showed an average moisture content of 3.92%, ash content of 1.17%, and an iodine adsorption capacity of 507.64 mg/g with an adsorption efficiency of 95.9557% and a cadmium adsorption capacity of 59.75 mg/g at a concentration of 20 ppm, pH 9, and a contact time of 40 minutes [13].

The activation process aims to increase or develop the volume and diameter of existing pores and also create new pores [14]. Activation not only increases the specific surface area of the pores and their active sites but also dissolves impurities in the material, thereby opening the pores further. This results in an increase in the specific surface area of the pores and an increase in the adsorption capacity of the biosorbent. The activation process can be carried out by applying chemical treatments such as the addition of acidic or basic compounds [7]. Research conducted by Rahman & Ishar (2023) activated matoa leaves with citric acid to adsorb Fe (III) metal; results were obtained under optimal conditions of pH 8, a contact time of 120 minutes, and a dose of 50 mg, achieving an efficiency of 78.43% [7]. Other studies, such as that conducted by Hanifah et al. (2024), activated white jabon fruit charcoal with NaOH to adsorb mercury (II) ions in water. The results showed that under optimal stirring conditions of 80 rpm during adsorption, an adsorption efficiency of 99.78% and an adsorption capacity of 0.9641 mg/g were achieved [15].

Based on this description, a study was conducted to determine the adsorption efficiency and capacity of NaOH-activated matoa fruit shell powder toward lead metal by varying adsorption parameters namely biosorbent dose, solution pH, pH_{pzc}, and contact time so that the adsorption process of lead (II) ions in the solution could reach optimal conditions.

2. RESEARCH METHODS

2.1. Preparation of Matoa Fruit Shell Samples

The samples used in this study were matoa fruit shells collected from Perawang Village, Tualang Subdistrict, Siak Regency, Riau Province. The matoa fruit shells were washed with distilled water until clean and dried under sunlight. The matoa fruit shells were ground using a chopper, then sieved using a 100-mesh sieve and retained on a 200-mesh sieve to obtain a homogeneous particle size, making them easier to process further during the activation stage.

2.2. Activation of Matoa Fruit Shells

The prepared samples were then activated using a 1 M NaOH solution with varying mass ratios of powder to NaOH solution, namely (1:1, 1:2, 1:3, 1:4, and 1:5) (w/v) in 250 mL beakers. For example, for each treatment, 30 grams of powder was used, so the volumes of NaOH solution used

were 30 mL, 60 mL, 90 mL, 120 mL, and 150 mL, respectively. The mixtures were stirred using a stirring rod for approximately 5 minutes and left to stand for 24 hours at room temperature. Afterward, each sample was washed with deionized water until the solution's pH became neutral, then filtered using Whatman No. 42 filter paper. The samples were then dried in an oven at 100±5°C for 24 hours and subsequently cooled in a desiccator. The dried samples were ready for characterization using FTIR and SEM-EDS and ready for application as biosorbents in the adsorption of lead(II) ions in solution.

2.3. Iodine Adsorption Capacity Test

A sample of matoa fruit shell powder was oven-dried at 100±5°C for 1 hour, then cooled in a desiccator for 30 minutes. A 0.5-gram sample was placed in a beaker containing 50 mL of 0.1 N iodine solution. The mixture was stirred using a magnetic stirrer for 15 minutes, then allowed to stand for 1 hour. The mixture was centrifuged for 15 minutes at 3000 rpm. A 5 mL aliquot of the supernatant from the centrifugation was taken for titration with 0.1 N $Na_2S_2O_3$until the solution turned pale yellow, then 1 mL of 1% starch solution was added as an indicator. Next, the titration was repeated until the observable endpoint was reached, marked by the disappearance of the blue color in the solution. The adsorption capacity of matoa fruit shells for iodine was calculated using Equation (1):

$$Adsorbed\ iodine\ \left(\frac{mg}{g}\right) = \frac{(V_1 \times N_1 - V_2 \times N_2) \times 126.9 \times fp}{W} \quad (1)$$

where V_1 is the volume of the analyzed iodine solution (ml), V_2 is the volume of sodium thiosulfate solution required (mL), N_1 is the normality of iodine (N), N_2 is the normality of sodium thiosulfate (N), W is the sample weight (g), and fp is the dilution factor.

2.4. Determination of the Optimal Biosorbent Dose

Samples were weighed with varying biosorbent masses of 0.01; 0.025; 0.05; 0.075; 0.1; 0.25; 0.5; 0.75, and 1.0 grams and mixed into 50 mL of a 20 ppm lead simulation solution. The mixture was stirred using a magnetic stirrer at 150 rpm for 60 minutes, then allowed to stand for 15 minutes. After that, the mixture was filtered using Whatman No. 42 filter paper. The filtrate was analyzed using ICP-OES.

2.5. Determination of Optimum pH and pH_{pzc}

The determination of the optimum pH was performed as follows. A sample was weighed to match the mass of the optimum biosorbent obtained and then mixed into 50 mL of 30 ppm lead simulation solution with varying pH values of 5, 6, 7, and 8. The mixture was stirred using a magnetic stirrer at 150 rpm for 60 minutes and then allowed to stand for 15 minutes. After that, the mixture is filtered using Whatman No. 42 filter paper. The filtrate is analyzed using ICP-OES.

The determination of the pH point of zero charge (pHpzc) was performed as follows. Twenty milliliters of 0.1 M NaCl solution was added to five separate 50 mL beakers with pH values of 3, 4, 5, 6, and 7. The pH of the solutions was adjusted using 0.1 M HCl and 0.1 M NaOH. Then, 0.1 grams of the sample was added to each solution and stirred using a magnetic stirrer at 150 rpm for 15 minutes. The mixtures were allowed to stand for 24 hours. The initial pH and final pH of each solution were measured, and a curve was plotted showing the relationship between ΔpH (pH change) versus pH0(initial pH). The pHpzc value for matoa fruit shell powder was obtained when ΔpH = 0. The measurement results were processed and interpreted in the form of tables and graphs using Microsoft Excel.

2.6. Determination of Optimum Contact Time

Samples were weighed to the optimum mass obtained and then mixed into 50 mL of 30 ppm lead simulation solution under the optimum pH conditions obtained. The mixtures were stirred using a magnetic stirrer at 150 rpm for varying durations of 20, 40, 60, and 80 minutes, then allowed to stand for 15 minutes. Afterward, the mixture was filtered using Whatman No. 42 filter paper. The filtrate was analyzed using ICP-OES.

The kinetic analysis of lead(II) ion adsorption was based on pseudo-first-order, pseudo-second-order, and intraparticle diffusion reaction kinetics to determine the interaction between the biosorbent and metal ions influenced by contact time.

The pseudo-first-order equation is expressed in Equation (2):

$$\frac{dq}{dt} = k_1(qe - qt) \tag{2}$$

Notes:
qe = Adsorption capacity at equilibrium (mg/g)
qt = Adsorption capacity at time t (mg/g)
k_1 = Pseudo-first-order rate constant (min^{-1})

The pseudo-second-order equation is expressed in Equation (3):

$$\frac{t}{qt} = \frac{1}{k_2 qe^2} + \frac{t}{qe} \tag{3}$$

Notes:
qe = Adsorption capacity at equilibrium (mg/g)
qt = Adsorption capacity at time t (mg/g)
k_2 = Pseudo-second-order rate constant ($g/mg \bullet min^{-1}$)

Intra-particle diffusion is described by the Weber-Morris equation (Equation 4):

$$q_t = k_d t^{\frac{1}{2}} \tag{4}$$

Notes:
q_t = Amount of adsorbate adsorbed at contact time t (mg/g)
k_d = Intraparticle diffusion rate constant ($mg/g \bullet min^{-1}$)
t = Contact time between the solute and the biosorbent (minutes)

The ½ exponent indicates that this model assumes the diffusion process controlling the adsorption rate is intraparticle diffusion.

3. RESULTS AND DISCUSSIONS

3.1. Characterization of CBM Powder with NaOH Activator Variations

The delignification process allows for the breakdown of the cellulose structure through the cleavage of glycosidic bonds [16]. This step is carried out using a NaOH solution because this strong base is capable of degrading the lignin structure. Activation with NaOH can dissolve the hemicellulose and lignin components of the biomass material, resulting in a more open porous structure. This significantly increases the active surface area of the biosorbent and enhances its adsorption capacity [17]. Additionally, NaOH plays a role in generating or increasing the number of functional groups such as hydroxyl (-OH) and carboxyl ($-COO^-$) on the biosorbent's surface. These groups are crucial in the adsorption process as they directly interact with pollutant molecules or ions, whether through ionic bonding, ion exchange, or electrostatic interactions [18]. The reaction of lignocellulose bond cleavage by NaOH is illustrated in Figure 1.

The reaction mechanism involves OH^- ions from NaOH breaking the bonds in the basic lignin structure, while Na^+ ions bind with lignin to form sodium phenolate. This phenolate salt is highly soluble [19]. This reaction causes the breaking of hydrogen bonds ( ) connecting lignin to cellulose and hemicellulose, as well as bonds between lignin and hemicellulose consisting of ether and ester groups and carbon-carbon bonds, resulting in lignin fragments [20]. Meanwhile, the degradation of lignin compounds by hydroxide ions from NaOH can be seen in Figure 2.

The lignin degradation reaction mechanism begins with the attack of a hydrogen atom bound to a phenolic OH group by a hydroxide (OH) ion from NaOH. Subsequently, a double bond forms between an O atom and a C atom in the phenolic group, and a shift in the conjugated double bond occurs. This triggers the breaking of the bond in the ether group, causing it to detach as R-OH. The

presence of dissolved lignin is indicated by the appearance of a dark black solution (black liquor). The appearance of this black color indicates that the dissolution of compounds containing chromophore groups—that is, groups with conjugated double bonds—enables the compound to absorb light with wavelengths ranging from 200 nm to 400 nm (UV) [20].

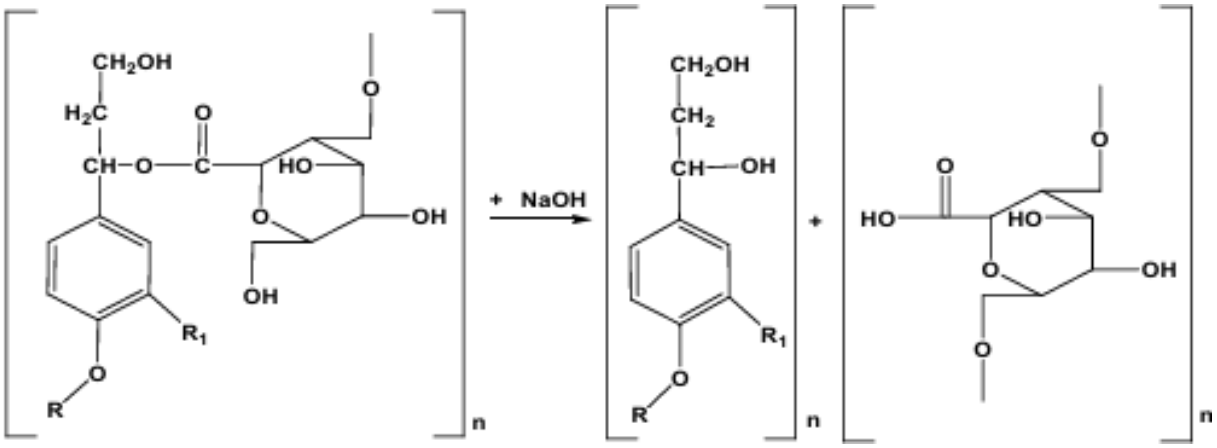

Figure 1. Reaction mechanism of lignocellulose bond cleavage by NaOH [20].

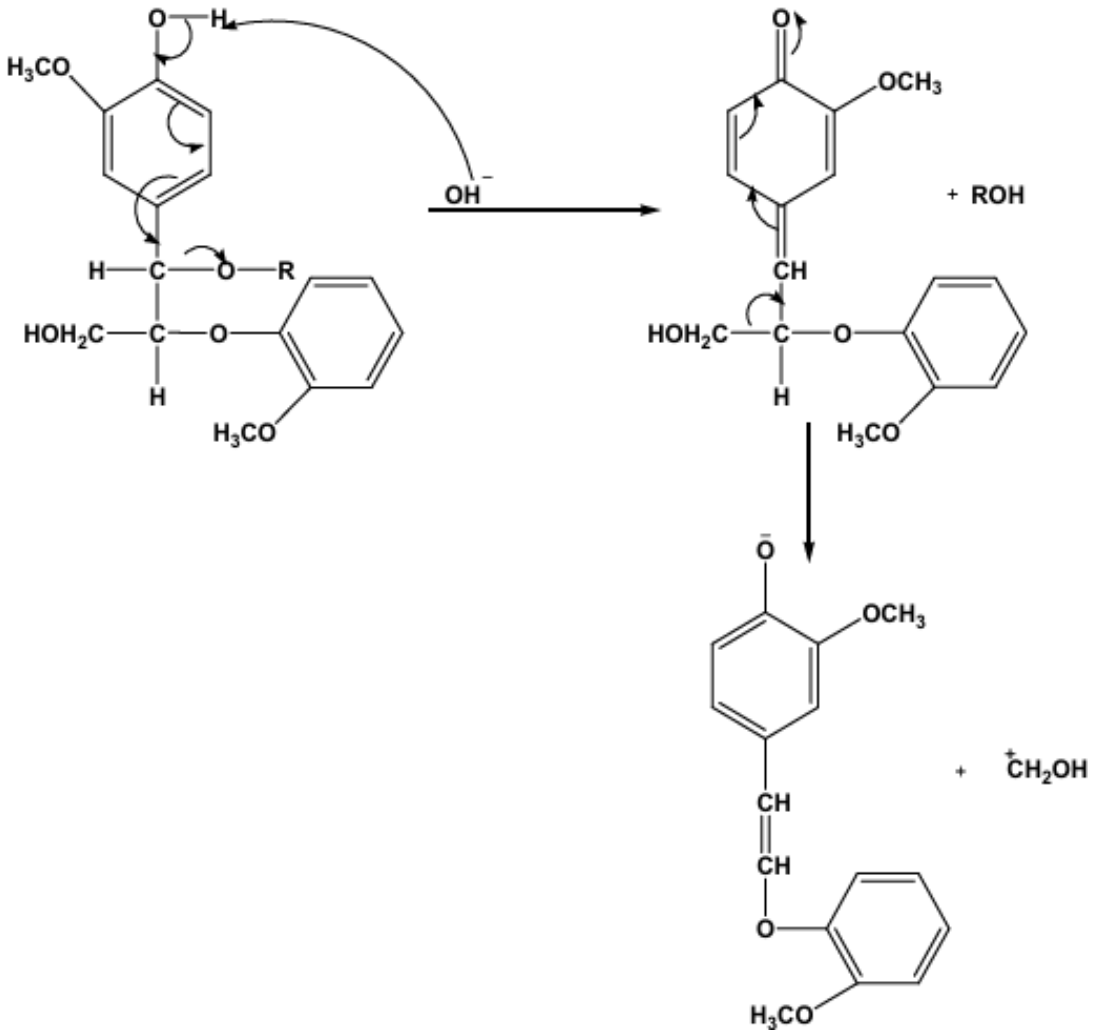

Figure 2. Reaction mechanism of lignin degradation [20].

3.2. Iodine Absorption Test

Characterization of CBM powder at various NaOH activation ratios: 1:1; 1:2; 1:3; 1:4; and 1:5. The characterization results are shown in Table 1.

Table 1. Characterization results of CBM powder at various NaOH activation ratios.

Activator ratio	Iodine adsorption capacity (mg/g)	Surface area (m^2/g)
1:1	329	27.31
1:2	373	30.96
1:3	177	14.69
1:4	217	18.01
1:5	233	19.34

Based on the results in Table 1, the iodine adsorption capacity at a 1:1 ratio was 329 mg/g and at a 1:2 ratio was 373 mg/g. This indicates that the higher the ratio of CBM powder to NaOH solution or, in other words, the more activator used the greater the iodine adsorption capacity, indicating that occur signifying an increase in the adsorption capacity of the CBM powder. Yuningsih et al. (2016) revealed that the greater the amount of activator used, the greater the formation of pores, resulting in increased porosity; this is due to the amount of impregnating agent used during the activation process [21]. The high iodine adsorption capacity demonstrates the formation of a greater number of microporous structures. According to Imelda et al. (2019), iodine adsorption capacity correlates with the surface area of the biosorbent. The higher the iodine number, the greater the surface area of the biosorbent, thereby increasing its ability to adsorb dissolved substances [22]. An increase in surface area is proportional to an increase in iodine adsorption capacity; this can be seen in the 1:1 ratio, which has a surface area of 27.31 m²/g, and the surface area further increases to 30.96 m²/g at the 1:2 ratio.

The highest iodine adsorption capacity in this study was observed at a 1:2 ratio, amounting to 373 mg/g. This value remains relatively low compared to the iodine adsorption capacity required by SNI 06-3730-1995, which stipulates a minimum of 750 mg/g. The low iodine adsorption capacity may be influenced by several factors, such as suboptimal activation or soaking processes and the presence of volatile compounds blocking the pores; therefore, it would be better to follow up with physical activation using heating to remove the volatile substances blocking the pores, thereby further improving the iodine adsorption capacity [23].

The mechanism of the iodine adsorption process begins when iodine molecules diffuse through a layer to the outer surface of the CBM powder, and part of the iodine solution continues to diffuse into the pores. CBM powder with high iodine adsorption capacity indicates a structure rich in micro- and mesopores. Iodine adsorption capacity analysis was performed using the iodometric titration method, wherein the iodine solution remaining after adsorption by the CBM powder serves as the titrand and is titrated with standardized sodium thiosulfate as the titrant, with the reaction occurring as follows [22]:

$$IO_3^- + 5I^- + 6H^+ \rightarrow 3I_2 + 3H_2O \quad (5)$$

$$I_2 + S_2O_3^{2-} \rightarrow 2I^- + S_4O_6^{2-} \quad (6)$$

Furthermore, the iodine adsorption capacities at ratios of 1:3, 1:4, and 1:5 were 177 mg/g, 217 mg/g, and 233 mg/g, respectively. These values indicate a decrease in iodine adsorption when the ratio of CBM powder to NaOH solution exceeds 1:2. The pore surface area of the CBM powder increases as the amount of added NaOH activator exceeds the 1:2 ratio. However, the formation of excessively large pores is expected to result in thinner pore walls that become brittle during washing. The brittleness of the pore walls has the potential to damage the pores, thereby further reducing their adsorption capacity. This decrease in the iodine number is caused by the addition of a sufficiently high concentration of NaOH solution, which can damage the formed microporous structure, resulting in a reduced number of pores and a decrease in pore surface area [24]. The decrease in surface area is proportional to the decrease in iodine adsorption capacity at a ratio exceeding 1:2; this can be observed

at ratios of 1:3, 1:4, and 1:5, which have surface areas of 14.69 m²/g, 18.01 m²/g,and 19.34 m²/g, respectively. Therefore, the greater the amount of activator used, the higher the iodine adsorption capacity; however, excessive use degrades or damages the cellulose, resulting in a decrease in adsorption capacity [25].

3.3. Morphological Analysis and Elemental Composition of NaOH-Activated CBM Powder Using SEM-EDS

The SEM characterization results of CBM powder before and after activation using NaOH are shown in Figure 3 at a magnification of 3000x.

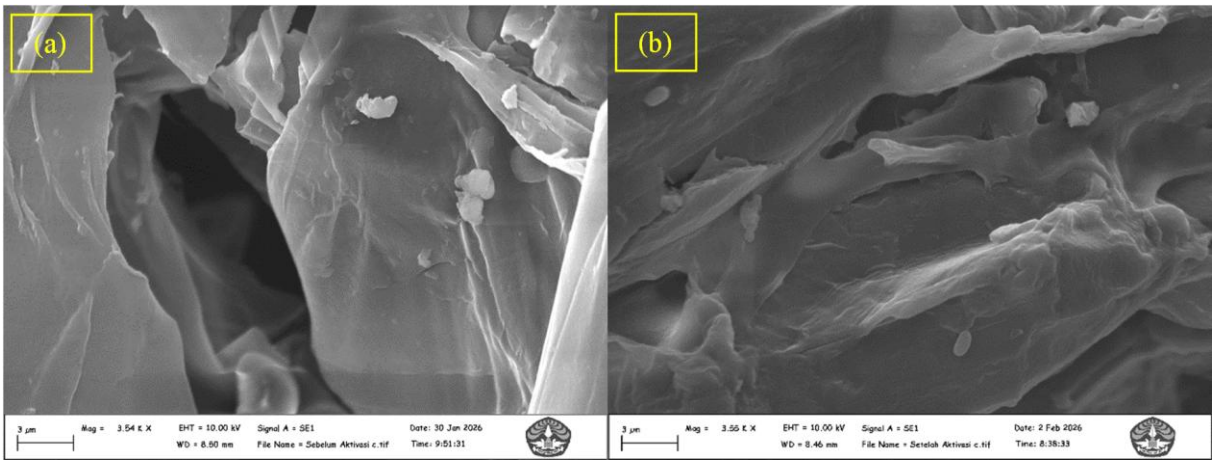

Figure 3. Surface morphology (a) of CBM powder before activation at 3000x magnification, (b) of CBM powder after activation at 3000x magnification.

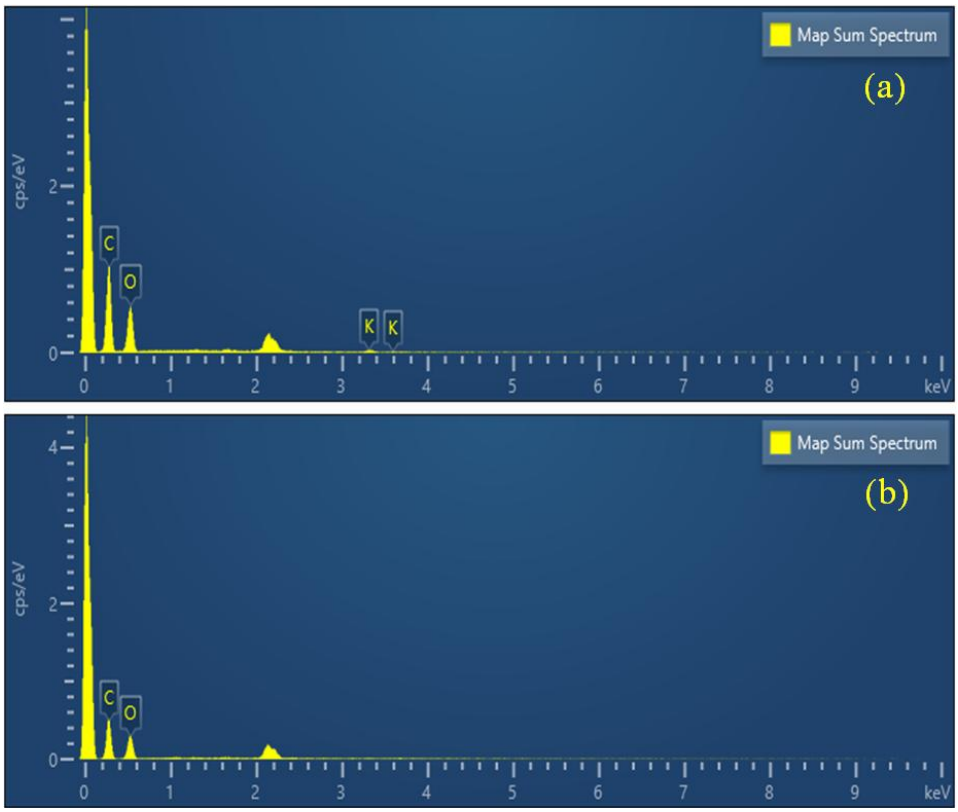

Figure 4. EDS spectra (a) of CBM powder before activation, (b) of CBM powder after activation.

Based on the SEM results in Figure 3, point (a) indicates that the surface morphology of the CBM powder before activation shows a limited number of micropores. Meanwhile, point (b) indicates that the surface morphology of the CBM powder after activation reveals small voids, indicating the formation of micropores and an increase in their number. The SEM characterization results indicate that activation by NaOH significantly influences changes in the morphological structure of CBM powder, both in terms of pore size and the formation of new pores. According to Evelin et al. (2018), during the chemical activation stage, the NaOH activator solution can interact with oxide compounds to erode impurities covering the pores [26]. Research conducted by Anwar et al. (2025) found that the release of lignin and other impurities by NaOH makes the biosorbent surface more porous, thereby providing a larger surface area compared to before activation [18]. A larger biosorbent surface area is known to enhance the biosorbent's ability to remove metal ions (Pb^{2+}) from solutions. A larger surface area provides more sites for the adsorption of lead (II) ions.

Table 2. Elemental composition of CBM powder before and after NaOH activation.

Element	Elemental composition (weight%)	
	Before activation	After activation
C	65.14	65.13
O	33.30	34.87
K	1.56	-
Total	100.00	100.00

The elemental composition of the CBM powder before and after activation was analyzed using the Energy Dispersive X-Ray Spectroscopy (EDS) method. The elemental composition of the CBM powder before and after NaOH activation is shown in Figure 4 and Table 2. The elemental composition before activation was carbon (C) 65.14%, oxygen (O) 33.30%, and potassium (K) 1.56%. Meanwhile, the elemental composition after activation was carbon (C) 65.13% and oxygen (O) 34.87%. Based on the EDS results, there was no significant change in the carbon and oxygen content; however, there was a loss of potassium minerals in the CBM powder following NaOH activation. The reduction in mineral salts may indicate the formation of $-COO^-$ and -OH functional groups on the biosorbent, thereby potentially enabling it to adsorb more Pb (II) ions [27]. The determination of these functional groups can be observed in the FTIR analysis.

3.4. FTIR Analysis of Functional Groups in NaOH-Activated CBM Powder

The functional groups of matoa fruit shell powder before activation, after activation, and after lead adsorption are shown in Table 3.

Table 3. Wavenumbers of CBM powder before activation, after activation, and after lead adsorption.

Functional groups	Wavenumber (cm^{-1})			
	Before activation	After activation	After adsorption	Indication
O–H stretching	3319.56	3270.55	3329.05	Cellulose
C–H sp^3 aliphatic	2921.44	-	2916.93	Cellulose
C–H aliphatic	2851.40	-	2850.98	Cellulose
C=O aldehyde	1723.93	-	-	Hemicellulose
C=C stretching aromatic ring	1603.91	-	-	Lignin
COOH	-	1593.02	1627.00	Cellulose
C–H bending	1318.00	1316.15	1315.26	Cellulose
C–O ester	1231.26	-	-	Lignocellulose
C–O ether	1158.05	1156.10	1158.59	Cellulose
C–O alcohol	1033.23	1029.61	1031.54	Cellulose
C–H aromatic	756.47	-	-	Lignin
Pb–O bending	-	-	698.32	Cellulose-lead

Based on Table 3, the analysis results show a cellulose hydroxyl (-OH) stretching group in the CBM powder before activation with a wavenumber of 3319.56 cm^{-1}, followed by a shift in the

wavenumber in the CBM powder after activation to 3270.55 cm^{-1} and in the CBM powder after adsorption to 3329.05 cm^{-1} [27].

Wavenumbers of 2921.44 cm^{-1} and 2851.40 cm^{-1} detected in the CBM powder before activation correspond to the aliphatic C-H groups of cellulose [27]. Meanwhile, these wavenumbers were not found in the CBM powder after activation, indicating the loss of aliphatic C-H bonds due to degradation by NaOH a sign that the activation was successful [27]. The wavenumber 1723.93 cm^{-1} indicates the presence of the aldehyde C=O carbonyl group from hemicellulose found in the CBM powder prior to activation [28]. The wavenumber 1603.91 cm^{-1} indicates the presence of the C=C stretching group of the aromatic ring from lignin in the CBM powder before activation [20].

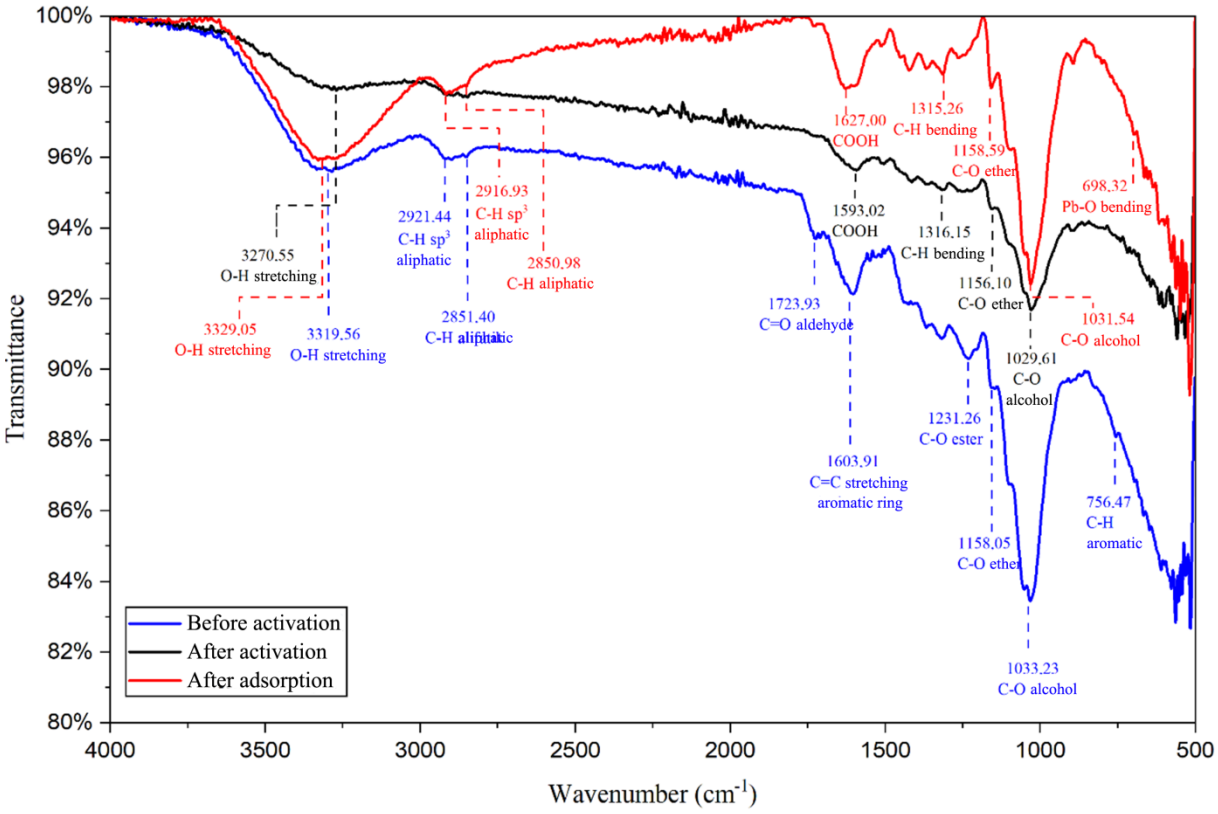

Figure 5. IR spectra of CBM powder before and after activation, as well as after lead adsorption.

Spectral analysis was performed using Fourier Transform Infrared (FTIR) for each biosorbent, as shown in Figure 5. In the CBM powder after activation, a new functional group appeared, marked by an absorption peak at a wavenumber of 1593.02 cm^{-1} indicating the formation of a carboxylate group (COOH) [28]. The wavenumber of 1318.00 cm^{-1} in the CBM powder before activation indicates the presence of C–H bending groups from cellulose; this is consistent with the study by Rambat et al. (2015), which found a wavenumber of 1319.31 cm^{-1} corresponding to C–H wagging in the bending category [20]. In the wavenumber range between 1179 – 1261 cm^{-1}, the wavenumber 1231.26 cm^{-1} is suspected to indicate the presence of C–O ester groups in the CBM powder prior to activation [28]. Research conducted by Quiroz et al. (2025) also found an O=C–O group at a wavenumber of 1241.2 cm^{-1} [29]. The wavenumber of 1158.05 cm^{-1} in the CBM powder prior to activation indicates the presence of a C–O ether group, which corresponds to the C–O stretching vibration of the cellulose backbone [29].

The wavenumber 1033.23 cm^{-1} in CBM powder before activation corresponds to the C–O alcohol group of cellulose [28]. The wavenumber 756.47 cm^{-1} in CBM powder before activation corresponds to the aromatic C–H group found in lignin [30]. The wavenumber 698.32 cm^{-1} is suspected to be a Pb–O group formed in the CBM powder after adsorption, indicating that an interaction has occurred between the CBM powder and Pb^{2+} ions. Arulmozhi & Mythili (2013) also identified Pb–O groups at wavenumbers of 686 cm^{-1} and 462 cm^{-1} [31].

3.5. Determination of the Optimal Biosorbent Dose for Lead (II) Ion Adsorption

The effect of biosorbent mass can be seen in the graph showing the relationship between biosorbent mass and adsorption efficiency in Figure 6.

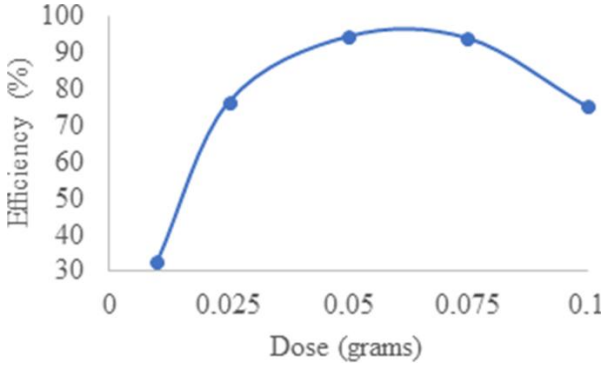

Figure 6. Graph showing the relationship between biosorbent dose and lead biosorption efficiency.

Based on the data in Figure 6, differences in biosorbent mass significantly affect the efficiency and adsorption capacity of lead (II) ions. As the biosorbent mass increases from 0.01 grams to 0.05 grams, adsorption efficiency increases significantly from 32.67% to 94.55%. Hanifah et al. (2023) noted that this aligns with the theory that a larger biosorbent mass results in an increased number of particles and surface area, thereby increasing the number of binding sites for metal ions and improving adsorption efficiency [32]. Additionally, an increase in biosorbent mass provides a greater number of active sites available for metal binding [28].

A biosorbent mass of 0.05 grams was selected as the optimal biosorbent mass because it showed the highest adsorption efficiency value in the graph based on Figure 6, this is because the remaining lead (II) ion concentration in the solution was the lowest, at only 1.1 ppm, when equilibrium was reached between the lead (II) ions and the activated CBM powder during the adsorption process, indicating that the biosorbent had maximally bound the adsorbate. When the biosorbent surface is saturated or nearly saturated with the adsorbate, two scenarios may occur: first, a second and subsequent adsorption layers form on top of the adsorbate already bound to the surface; this phenomenon is known as multilayer adsorption. Meanwhile, the second scenario involves no formation of a second or subsequent layers, so the unadsorbed adsorbate diffuses out of the surface pores and returns to the fluid stream [33].

At a dose of 0.075 grams, the adsorption efficiency remains high at 94.06%, but as the dose increases, the efficiency decreases, reaching only 18.33% at 1 gram. This decrease in adsorption efficiency may be caused by overlapping during the adsorption process due to biosorbent agglomeration, which reduces the surface area of the biosorbent as surface pores are covered by adjacent biosorbent particles, thereby decreasing the number of active sites [34]. Anwar et al. (2022) also stated that the decrease in adsorption capacity with an increase in biosorbent mass is caused by the aggregation of biosorbent particles, which leads to a reduction in surface area. The aggregation of biosorbent particles also causes the desorption of weakly bound adsorbates from the biosorbent surface [35].

3.6. Determination of the Optimum pH for Lead (II) Ion Adsorption and Determination of the pH_{pzc} of NaOH-Activated CBM Powder

The effect of pH can be seen in the graph showing the relationship between pH and adsorption efficiency in Figure 7.

Based on the graph in Figure 7, it is evident that there is an increase in the amount of lead (II) ions adsorbed by the CBM powder, as indicated by a rise in adsorption efficiency from 88.62% at pH 5 to 89.87% at pH 6. The adsorption capacity also showed a value of 26.94 mg/g at pH 5, which then increased to 27.32 mg/g at pH 6. The low adsorption efficiency and capacity at pH values below 6 are due to the fact that at lower pH conditions which are too acidic there is a high concentration of H^+ ions, leading to competition between H^+ ions and lead (II) ions (which are also positively charged) to

bind with the free electron pairs of the active groups on the biosorbent. Furthermore, lower pH conditions can cause electrostatic repulsion between CBM powder and lead(II) ions because the active groups on the biosorbent surface undergo protonation, resulting in only a small fraction of lead ions being adsorbed [36].

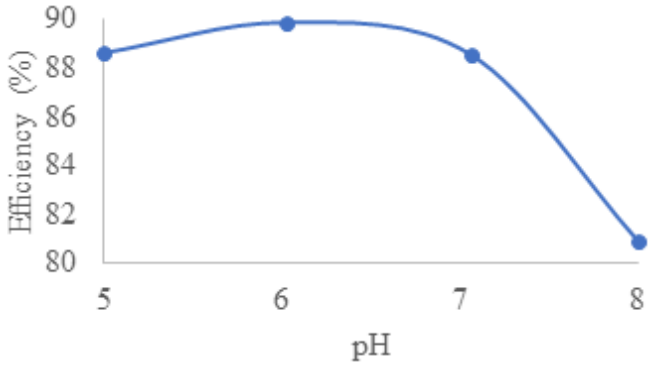

Figure 7. Graph showing the relationship between pH and lead biosorption efficiency.

The highest adsorption efficiency and capacity values indicate that pH 6 is the optimum pH in this study. Deprotonation resulting from the increase in pH up to pH 6 also caused the biosorbent to undergo a change in the surface charge of the CBM powder, making it more negatively charged and thus more capable of binding lead (II) ions, which were successfully adsorbed to the maximum extent by the CBM powder [37]. A gradual increase in pH leads to the formation of complex ions [38]. According to Sihotang (2021), the interaction between metal ions and the -OH groups of cellulose can occur through a coordination complex formation mechanism because the oxygen (O) atom in the -OH group has a lone pair of electrons, while the metal ion has an empty d orbital. These unpaired electrons will occupy the empty orbitals of the metal ions, thereby forming a compound or complex ion [37].

Adsorption efficiency decreases at pH 7 and pH 8, reaching 88.55% and 80.92%, respectively. This occurs because at higher pH conditions, there are more OH^- ions, leading to precipitation the formation of $Pb(OH)_2$ precipitate from the reaction between Pb^{2+} ions and OH^- ions. This precipitate can then cover the pores and active sites on the surface of the CBM powder, thereby hindering the adsorption process of lead (II) ions, which causes the adsorption efficiency to decrease [36]. The same trend is observed in adsorption capacity at pH 7 and pH 8, which decrease successively as pH increases, reaching 26.92 mg/g and 24.60 mg/g, respectively. Several previous studies using varying pH parameters reported an optimal pH of 4, consistent with this study. For instance, Zein et al. (2019) used kapok fruit peel to adsorb lead (II) ions with a capacity of 223.72 mg/g [38], and Hanifah et al. (2023) used salak peel to adsorb lead (II) ions with an efficiency of 93.36% [32], and Sihotang (2021) used sago palm peel to adsorb lead (II) ions in textile wastewater with an efficiency of 99.91% and a capacity of 1.5879 mg/g [37].

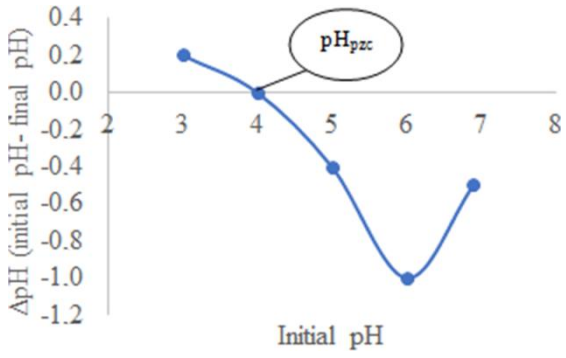

Figure 8. pH_{pzc} graph for NaOH-activated CBM powder.

The pHpzcvalue is the pH at which the surface charge of the biosorbent is zero. The pH_{pzc} value is determined from the intersection point between the straight line of the initial pH curve and ΔpH (initial pH – final pH) [39]. The pH_{pzc} graph is presented in Figure 8, showing that the pH_{pzc} value is at pH 4 because at that pH, the intersection point lies on the x-axis line connecting the initial pH to ΔpH. The pH_{pzc} condition at pH 4 indicates that at that point, the surface charge of the CBM powder has an equal number of positive charges as negative charges. If pH < pH_{pzc} (below pH 4), the surface of the CBM powder is positively charged, resulting in electrostatic repulsion with lead (II) ions (which are cations), leading to low adsorption capacity. The theory states that at pH values below pH_{pzc}, the biosorbent surface is dominated by positive charges [40]. When pH > pH_{pzc} (above pH 4), the surface of the CBM powder is negatively charged, resulting in electrostatic attraction with lead (II) ions, which increases its adsorption capacity. This is evidenced by the fact that the optimal pH (pH 6) is higher than pH_{pzc}, indicating that the surface charge at pH 6 is negative, allowing it to bind more lead (II) ions with the highest adsorption efficiency. According to Zein et al. (2023), the biosorbent surface has a negative charge if pH > pH_{pzc} due to the deprotonation of functional groups such as OH^- and COO^-, making it suitable for the adsorption of cationic substances [39].

3.7. Determination of the Optimum Contact Time for Lead (II) Ion Adsorption and Determination of the Adsorption Kinetic Model

The effect of contact time can be seen in the graph showing the relationship between contact time and adsorption efficiency in Figure 9.

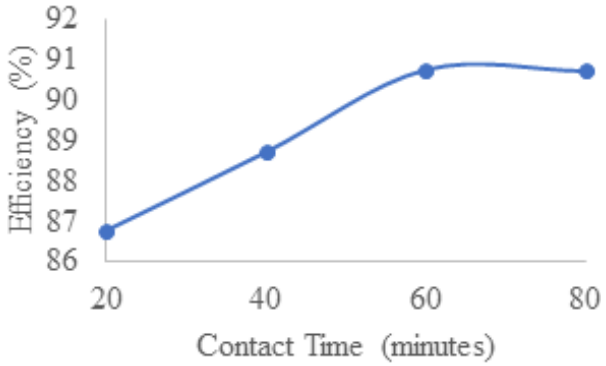

Figure 9. Graph showing the relationship between contact time and lead biosorption efficiency.

As shown in Figure 9, the adsorption efficiency at a contact time of 20 minutes was 86.78%; This is because, at a contact time of 20 minutes, not all of the hydroxyl (-OH) groups of the cellulose biosorbent have bonded with lead(II) ions, so the amount of lead(II) ions adsorbed by the pores of the CBM powder is not yet maximal [37]. Subsequently, the adsorption efficiency increases as the contact time increases, reaching 90.76% at 60 minutes. The longer the contact time, the longer the interaction between the biosorbent and the adsorbate, allowing more opportunities for lead (II) ions to come into contact with the CBM powder and form bonds that fill the surface pores, resulting in a greater number of adsorbed lead (II) ions [32]. Additionally, increasing contact time enhances the likelihood of functional groups on the biosorbent interacting with metal ions [30]. Adsorption capacity also showed an increase as contact time increased from 26.38 mg/g at 20 minutes to 27.59 mg/g at 60 minutes.

After reaching 60 minutes, adsorption efficiency tends to stabilize and even slightly decreases at 80 minutes, with an efficiency of 90.72% and an adsorption capacity of 27.58 mg/g. This is because the amount of CBM powder bound to lead (II) ions has reached saturation. The saturation of CBM powder in adsorbing lead (II) ions upon reaching equilibrium indicates that nearly all active sites on the CBM powder have already bound, making further extension of time ineffective. This is a phenomenon in physical adsorption stating that the adsorption process is reversible due to weak bonds between the biosorbent and lead (II) ions, causing lead (II) ions on the biosorbent surface to be released back into the solution as contact time increases [35]. Additionally, the decrease in adsorption capacity is due to the pores of the CBM powder becoming fully filled, causing the surface to become

saturated and reducing its adsorption capacity [30]. Therefore, the optimal contact time in this study is 60 minutes, with an efficiency of 90.76% and a capacity of 27.59 mg/g.

Previous studies that varied contact time parameters, such as those conducted by Dewi et al. (2015), used plantain peel to adsorb lead (II) ions for 20 minutes with an adsorption capacity of 2.8936 mg/g [24], and Kustomo et al. (2022) used matoa fruit peel to adsorb cadmium (II) ions for 40 minutes with an efficiency of 69.4943% and an adsorption capacity of 59.75 mg/g [41]. Meanwhile, a study in which the optimal contact time was obtained similarly to this study was conducted by Anwar et al. (2022) using Siamese orange peel for the adsorption of mercury (II) ions over 60 minutes with an efficiency of 78.51% [35], and the study by Simbolon et al. (2022) utilized coconut husk to adsorb iron from leachate over 60 minutes with an efficiency of 30.84% [42].

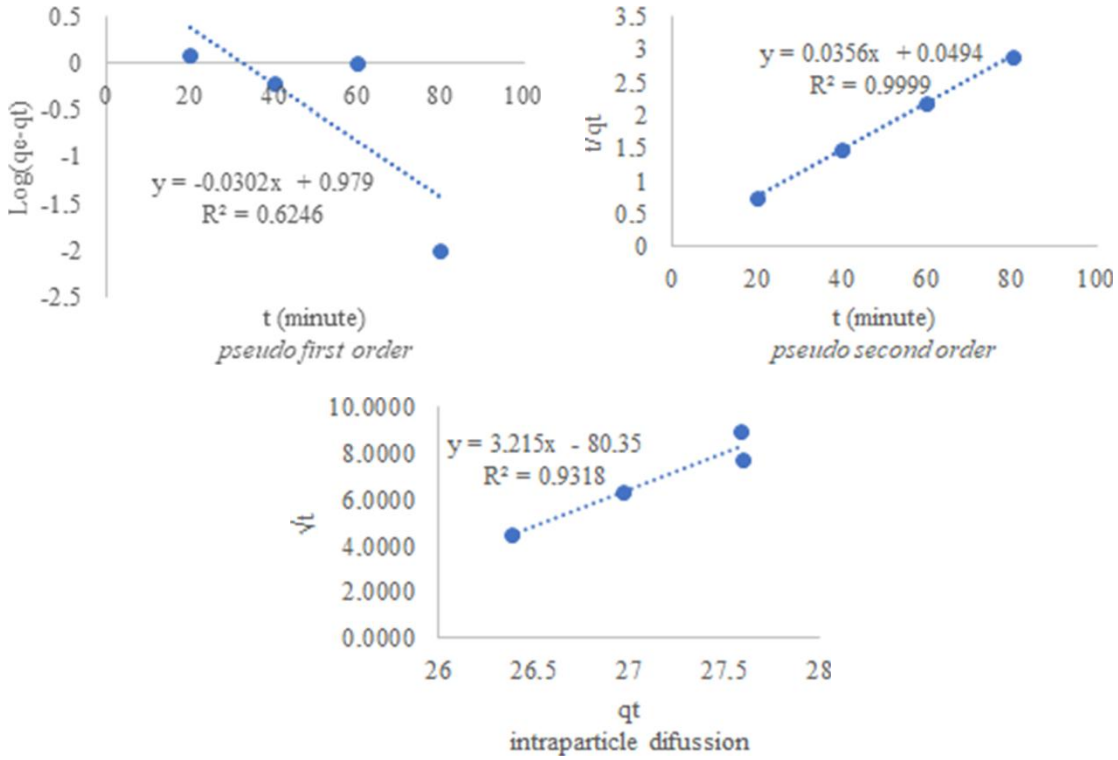

Figure 10. Graphs of the pseudo-first-order, pseudo-second-order, and intraparticle diffusion adsorption kinetic models.

Table 4. Comparison of the three adsorption kinetic models.

Model	Rate constant	Theoretical qt (mg/g)	Experimental qe (mg/g)	R^2	Fit
First-order pseudo-fit	0.0695 min^{-1}	9.53	27.59	0.6246	Does not fit
Pseudo-second order	0.0256 g/mg.min	28.09	27.59	0.9999	Very good fit
Intraparticle diffusion	0.311 mg/g.$min^{1/2}$	27.77	27.59	0.9318	Supporting mechanism

Chemical kinetics is the science of reaction rates and the processes by which reactions occur [40]. The determination of adsorption kinetics aims to determine the rate of adsorption of metal ions [41]. The adsorption kinetics model was determined by plotting curves using three models: pseudo-first order, pseudo-second order, and intraparticle diffusion. A comparison of the three adsorption kinetics models using NaOH-activated CBM powder is shown in Table 4. Based on the results of the curves, the first-order pseudo-model yielded a linear regression equation of y = -0,0302x + 0,979. The reaction rate constant (k_1) is 0.0695 min^{-1} with a very low linear regression coefficient (R^2) of 0.6246.

The adsorption capacity obtained from the first-order pseudo-model is 9.53 mg/g. The calculation results show that thetheoretical qe is much smaller than the experimental qe,with a very large difference of 18.06, or about 65% of the experimental qevalue. This indicates that the first-order pseudo-model is not suitable for describing lead (II) ion adsorption.

The pseudo-second-order model yielded a regression equation of y = -0,0356x + 0,0494. The reaction rate constant (k_2) is 0.0256 g/mg•min, with a linear regression coefficient (R^2) approaching 1, specifically 0.9999. The adsorption capacity obtained from the pseudo second order model is 28.09 mg/g, which is very close to the adsorption capacity in this study, which is 27.59 mg/g. The calculation results show that the theoretical qe and experimental qe values are very close, with a very small difference of 0.5 mg/g. This indicates that the pseudo second order model is more representative in explaining the adsorption kinetics of lead (II) ions because it yields theoretical and experimental qe values that are not significantly different from each other and has a much higher coefficient of determination compared to the pseudo first order model. According to Huang et al. (2014), if the kinetic model for adsorption better fits the pseudo-second-order kinetic model, then the adsorption occurring is a chemical adsorption process (chemisorption) that is, adsorption involving chemical interactions between the active sites of the biosorbent (CBM powder) and the adsorbate (lead (II) ions) so that the adsorbate cannot move freely to other parts [43].

The intraparticle diffusion model yielded a regression equation of y = 3.215x – 80.35. The reaction rate constant (ki) is 0.311 mg/g•$min^{1/2}$, with a sufficiently good linear regression coefficient (R^2) of 0.9318, though still lower than that of the pseudo-second-order model (0.9999). The adsorption capacity obtained from intraparticle diffusion is 27.77 mg/g, which is very close to the adsorption capacity in this study, which is 27.59 mg/g. The calculation results show that the theoretical qe and experimental qe values are very close, with a very small difference of 0.18 mg/g. This indicates the influence of intraparticle diffusion during the initial stage of adsorption; however, it is not the sole rate-controlling mechanism and serves only as a supporting mechanism during the adsorption process.

4. CONCLUSION

Based on the research results, the NaOH-activated matoa fruit shell (*Pometia pinnata*) powder biosorbent showed good potential for adsorbing lead (II) ions from solution. Characterization results indicated that the biosorbent had an iodine adsorption capacity of 373 mg/g with a surface area of 30.96 m^2/g. Optimal biosorption conditions were achieved at a biosorbent mass of 0.05 grams, pH 6, and a contact time of 60 minutes, with an adsorption efficiency of 90.76% and an adsorption capacity of 27.59 mg/g. FTIR analysis indicated the involvement of hydroxyl (-OH) and carboxyl ($-COO^-$) groups in the lead(II) ion binding process. Furthermore, the adsorption kinetics data followed a pseudo-second-order equation model (y = 0.0356x + 0.0494, R^2 = 0.9999), indicating that the adsorption mechanism is dominated by chemisorption. The results of this study indicate that NaOH-activated matoa fruit shell biosorbents have the potential to be used as an environmentally friendly alternative adsorbent for the treatment of lead-containing wastewater.

REFERENCES

[1] Anggari, W. (2016). Pemanfaatan Daun Matoa (*Pometia pinnata*) Sebagai Biosorben Ion Logam Tembaga (Cu) Dalam Air Menggunakan Aktivator Asam Sitrat. *Skripsi*. Universitas Islam Indonesia, Yogyakarta.

[2] Yuniastuti, E., Yuliana, A., Sukaya, & Nandariyah. (2023). Genetic diversity of matoa (*pometia pinnata*) species based on rapd markers. *SABRAO Journal of Breeding and Genetics*, **55**(6), 1941–1949.

[3] Setyawan, D. (2019). Uji Aktivitas Antibakteri Dari Daging Buah Matoa (*Pometia Pinnataj. R & G.Forst*) Terhadap Bakteri *Staphylococcus Aureus* Dan *Escherichia Coli*. *Skripsi*. Institut Kesehatan Helvetia, Medan.

[4] Rahmawati R., Tahir M., & Amir A. H. W. (2021). Kimia kandungan senyawa dan aktivitas farmakologis tanaman matoa (*Pometia pinnata JR Forster & JG Forster*). *Sci. J. As-Syif*, **13**(2), 108–115.

[5] Pakaya, M. S., Nazwah, B. P.K., Santi, Nurdiandra, J., Made, I. H. W., & Fajar, D. A. (2021). Pemanfaatan limbah kulit buah matoa (*pometia pinnata*) sebagai obat kumur herbal solusi pencegah karies gigi. *Jurnal Sibermas (Sinergi Pemberdayaan Masyarakat)*, 570–580.
[6] Faustina, F.C. & Santoso, F. (2014). Extraction of fruit peels of pometia pinnata and its antioxidant antimicrobial activities. *J. Pascapanen*, **11**(2), 80–88.
[7] Rahman, A. A. & Ishar, M. D. (2023). Pengaruh pH terhadap kemampuan absorben daun matoa menyerap logam Fe (III). *Jurnal Teknologi Terapan*, **7**(3), 1110–1117.
[8] Kurniawan, H., Calvin, H. G., Aning, A., & Antaresti. (2017). Pemanfaatan kulit buah matoa sebagai kertas serat campuran melalui proses pretreatment dengan bantuan gelombang mikro dan ultrasonik. *Jurnal Ilmiah Widya Teknik*, **16**(1), 1–10.
[9] Zustriani, A. K. & Naila, L. Z. F. (2023). Adsorpsi logam Cd pada limbah cair laboratorium menggunakan biosorben arang aktif dari kulit buah matoa. *Integrated Lab Journal*, **11**(1), 50–60.
[10] Astuti, W. & Bayu, K. (2015). Adsorpsi Pb^{2+} dalam limbah cair artifisial menggunakan sistem adsorpsi kolom dengan bahan isian abu layang batubara serbuk dan granular. *Jurnal Bahan Alam Terbarukan*, **4**(1), 27–33.
[11] Hughes, M. & Poule, R. K. (1984). *Metals and Microorganism*. Chapman and Hall, London.
[12] Safrianti, I., Nelly, W., & Titin, A. Z. (2012). Adsorpsi timbal (II) oleh selulosa limbah jerami padi teraktivasi asam nitrat: pengaruh pH dan waktu kontak. *Jurnal Kimia Khatulistiwa*, **1**(1), 1–7.
[13] Faza, N. L. Z. (2021). Adsorpsi Logam Cd(II) Menggunakan Biosorben Arang Aktif Dari Kulit Buah Matoa Teraktivasi Asam Nitrat. *Skripsi*. Universitas Islam Negeri Walisongo, Semarang.
[14] Serrano, V. G., Villegas, J. P., Florindo, A. P., Valle, C. D., & Calahorro, C. V. (1996). FT-IR study of rockrose and of char and activated carbon. *Journal of Analytical and Applied Pyrolysis*, **36**(1), 71–80.
[15] Hanifah, T. A., Sofia, A., Itnawita, Ganis, F. K., & Romauli. (2024). Biosorben arang buah jabon putih (*anthocephalus cadamba miq.*) untuk menjerap ion logam merkuri (II) dalam air. *Jurnal Senpling Multidisiplin Indonesia*, **2**(2), 49–55.
[16] Afifah, D. N., Adam, M., Tantri, A. S., & Ardi, W. (2024). Optimasi delignifikasi kulit singkong (*manihot esculenta*) dengan pelarut basa naoh menggunakan metode response surface methodology (RSM). *Jurnal Techno*, **25**(1), 63–72.
[17] Zhu, Z., Zheng, H., Wang, N., Wang, K., & Wu, Y. (2010). Preparation and characterization of NaOH activated carbon from sawdust for removing lead ion from wastewater. *Chemical Engineering Journal*, **158**(3), 544–551.
[18] Anwar, H., Devi, K. S., Miftahul, D., & Dina, E. R. (2025). Perbandingan efektivitas adsorpsi ion logam timbal (Pb) menggunakan biji buah durian teraktivasi NaOH dan HCl. *Jurnal Redoks*, **10**(1), 65–72.
[19] Purwiandono, G., Puji, L., Wahyu, W., Marlina, & Nadia, A. (2017). Adsorption isotherm studies of rhodamine B on citrus sinesis peel. *Indonesian Journal of Chemical Research*, **2**(1-2), 47–53.
[20] Rambat, Nurul, H. A., & Bambang, R. (2015). Aplikasi limbah kulit buah kakao sebagai media fermentasi asam laktat untuk bahan baku bioplastik. *Jurnal Kimia dan Kemasan*, **37**(2), 111–122.
[21] Yuningsih, L. M., Dikdik, M., & Jaka, A. K. (2016). Pengaruh aktivasi arang aktif dari tongkol jagung dan tempurung kelapa terhadap luas permukaan dan daya jerap iodin. *Jurnal Kimia VALENSI: Jurnal Penelitian dan Pengembangan Ilmu Kimia*, **2**(1), 30–34.
[22] Imelda, D., Amalia, K., & Dita, W. (2019). Pengaruh ukuran partikel dan suhu terhadap penyerapan logam tembaga (Cu) dengan arang aktif dari kulit pisang kepok (*musa paradisiaca formatypica*). *Jurnal Teknologi*, **6**(2), 107–118.
[23] Sari, F., Gema, F., Syamsudin, A. B., Athiek, S. R., & Hera, H. (2022). Pengaruh pH dan waktu terhadap adsorpsi logam timbal (Pb) dengan arang aktif dari gambas (*luffa acutangula*) atau oyong kering. *Jurnal Konversi*, **11**(1), 31–37.
[24] Dewi, M. S., Eko, B. S., & Endang, S. (2015). Pemanfaatan arang aktif kulit pisang raja untuk menurunkan kadar ion Pb(II). *Indonesian Journal of Chemical Science*, **4**(3), 228–233.

[25] Ganing, M. (2022). Pengaruh konsentrasi aktivator NaOH pada arang aktif tongkol jagung terhadap adsorpsi ion Pb^{2+}. *Jurnal Teknologi Kimia Mineral*, **1**(2), 76–80.
[26] Evelin, L. S., Irfana, D. F., & Joko, S. (2018). Aplikasi metode fraktal untuk karakterisasi struktur mikroskopik karbon aktif limbah tandan sawit teraktivasi NaOH. *Prisma Fisika*, **6**(1), 39–43.
[27] Purwiandono, G. & Army, S. H. (2022). Studi adsorpsi logam Pb(II) menggunakan biosorben kulit rambutan teraktivasi HNO_3 dan NaOH. *Indonesian Journal of Chemical Research*, **7**(1), 8–16.
[28] Wattanakornsiri, A., Pitchayanin, R., Thatiya, S., Suphapan, S., Tongsai, J., & Pongthipun, P. (2022). Local fruit peel biosorbents for lead(II) and cadmium(II) ion removal from waste aqueous solution: a kinetic and equilibrium study. *South African Journal of Chemical Engineering*, **42**, 306–317.
[29] Quiroz, G. E. T., Selene, A. V. L., Adriana, V. G., Ruth, A. C. V., Ramiro, E. G., & Raul, C. M. (2025). Surfactant-enhanced guava seed biosorbent for lead and cadmium removal: kinetics, thermodynamics, and reusability insights. *Sustainable Chemistry*, **6**(5), 1–34.
[30] Batu, M. S., Emerensiana, N., & Maria, M. K. (2022). Pembuatan karbon aktif dari limbah sabut pinang asal pulau timor sebagai biosorben logam Ca dan Mg dalam air tanah. *Jurnal Integrasi Proses*, **11**(1), 21–25.
[31] Arulmozhi, K. T. & Mythili, N. (2013). Studies on the chemical synthesis and characterization of lead oxide nanoparticles with different organic capping agents. *AIP Advances*, **3**, 1–9.
[32] Hanifah, H. N., Ginayanti, H., & Lisna, D. (2023). Potensi karbon aktif kulit salak (*salacca zalacca*) sebagai biobiosorben logam timbal (Pb) dari limbah laboratorium farmasi. *Kimia Padjadjaran*, **1**(2), 85–94.
[33] Arini, G. A. & Aminah, S. (2020). Pemanfaatan serbuk gergaji kayu jati (*tectona grandis l.f*) sebagai biosorben logam Cu(II). *Media Eksakta*, **16**(2), 89–97.
[34] Putri, R. K., Bohari, Y., & Nanang, T. W. (2025). Adsorpsi zat warna direk hitam menggunakan arang aktif dari mahkota nanas (*ananas comosus (l) merr*) termodifikasi kitosan. *Jurnal Atomik*, **10**(1), 50–60.
[35] Anwar, N. A. F., Ika, M., & Dwi, E. R. (2022). Pengaruh variasi waktu kontak dan massa biosorben kulit jeruk siam (*citrus nobilis*) terhadap penyisihan kadmium (Cd) dan merkuri (Hg). *Jurnal Teknologi Lingkungan UNMUL*, **6**(1), 35–43.
[36] Neolaka, Y. A. B. (2020). Studi optimasi pH dan massa adsorpsi ion logam Pb(II) dari sampel air menggunakan karbon aktif dari kayu kesambi (*schlecera oleosa*). *Prosiding Webinar Nasional Pendidikan dan Sains Kimia 3*, 129–133.
[37] Sihotang, R. (2021). Pengaruh larutan aktivator, waktu kontak dan pH larutan dalam pembuatan biosorben kulit buah aren (*arenga pinnata*) untuk adsorpsi timbal dalam limbah cair tekstil. *Syntax Idea*, **3**(5), 1175–1193.
[38] Zein, R., Dewi, N., Refilda, & Hermansyah, A. (2019). Penyerapan timbal(II) dan cadmium(II) di dalam larutan menggunakan limbah kulit buah kapuk. *Chimica et Natura Acta*, **7**(1), 37–45.
[39] Zein, R., Indah, T. M., Emriadi, Putri, R., & Syiffa Fauzia. (2023). Potensi biosorben kulit batang sagu (*metroxylon sago*) untuk penyerapan zat warna crystal violet: studi isoterm, kinetika, termodinamika dan aplikasi. *Journal of The Indonesian Society of Integrated Chemistry*, **15**(2), 83–98.
[40] Zein, R., Novrizaldi, W., Refilda, & Hermansyah, A. (2018). Kulit Salak sebagai biosorben potensial untuk pengolahan timbal(II) dan cadmium(II) dalam larutan. *Chimica et Natura Acta*, **6**(2), 56–64.
[41] Kustomo, Naila, L. Z. F., & Andreas, H. (2022). Adsorption of Cd (II) into activated charcoal from matoa fruit peel. *Walisongo Journal of Chemistry*, **5**(1), 83–93.
[42] Simbolon, L. A., Budi, N. W., & Edhi, S. (2022). Pemanfaatan sabut kelapa sebagai biobiosorben untuk penurunan konsentrasi besi (Fe) dan kromium (Cr) air lindi dengan variasi waktu kontak dan kecepatan pengadukan menggunakan sistem batch. *Jurnal Teknologi Lingkungan UNMUL*, **6**(1), 12–24.
[43] Huang, Y., Li, S., Chen, J., Zhang, X., & Chen, Y. (2014). Adsorption of Pb(II) on mesoporous activated carbons fabricated from water hyacinth using H_3PO_4 activation: Adsorption capacity, kinetic and isotherm studies. *Applied Surface Science*, **293**, 160–168.